ADVANCED FUNCTIONAL MATERIALS

www.afm-journal.de

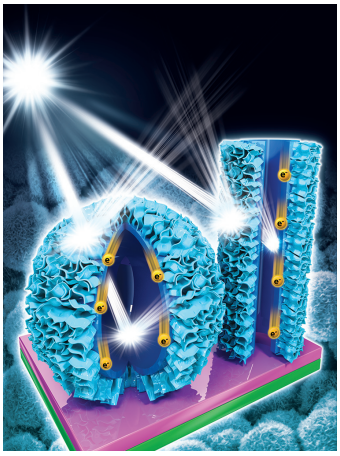

Solar Cells

J. H. Kim and co-workers present an effective method to prepare hierarchical double-shell nanostructures consisting of TiO_2 nanosheets on SnO_2 hollow spheres. On page 5037, these nanostructures display a large surface area, excellent electron transport, and improved light scattering. The resulting dye-sensitized solar cells with a solid electrolyte show an enhanced efficiency of up to 8.2% at 100 mW cm^{-2}.

Selective Adsorption

A nanoporous polymer network based on reactive smectic liquid crystals is used as an efficient and selective adsorbent. The inside cover image shows the selective adsorption of a blue dye from a mixture of dyes, described in detail on page 5045 by D. J. Broer, A. P. H. J. Schenning, and co-workers. The dye can be released and the adsorbent can be re-used. Cover design by ICMS Animation Studio TU/e.

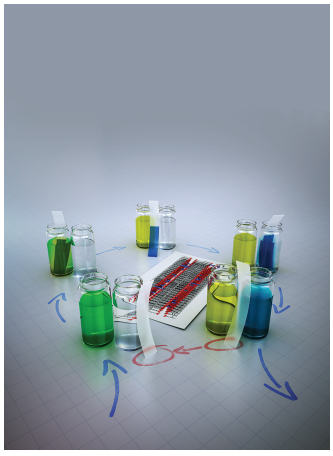

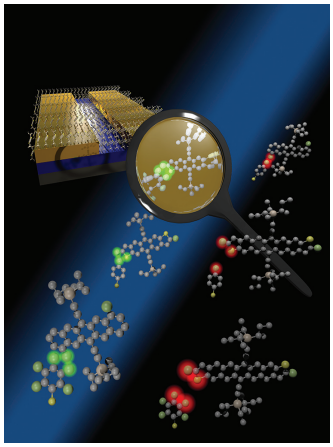

Organic Semiconductors

Halogen–halogen and halogen–sulphur interactions at the interface between a semiconductor and self-assembled monolayer-treated contacts can mediate film crystallization in organic thin-film transistors. On page 5052, A. Amassian, O. D. Jurchescu, and co-workers explain how highly ordered films form when such interactions are allowed by the structure and orientation of the consituent molecules during the heterogenous nucleation at the solution–solid interface.

FULL PAPERS

Invisible Inks

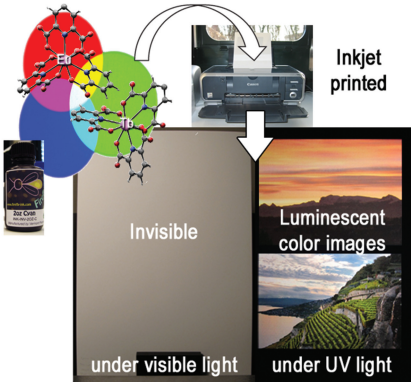

Europium and terbium trisdipicoliate complexes are used as luminescent inks and inkjet printed onto paper with a blue-emitting ink in order to obtain invisible luminescent full color images. This study describes the synthesis of the proposed lanthanide-based inks and the corresponding color reproduction workflow. These images are only reproducible by using the appropriate luminescent inks and software.

Solar Cells

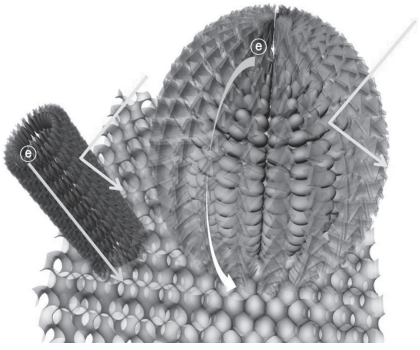

Hierarchical double-shell nanostructures consisting of TiO_2 nanosheets on SnO_2 hollow spheres are prepared to provide large surface area, excellent electron transport, and improved light scattering. The resulting solid-state dye-sensitized solar cells show enhanced efficiency up to 8.2% at 100 mW cm^{-2}, one of the highest values observed for N719 dye.

Selective Adsorption

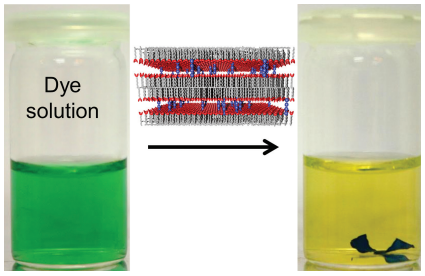

Selective and efficient adsorption is achieved with a porous nanostructured liquid crystalline polymer network. The confined pore dimensions allow charge and size selective adsorption and the smectic porous nature results in fast accessibility of all adsorption sites.

Organic Semiconductors

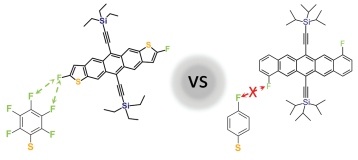

The role of interfacial halogenation in mediating texture formation and the self-patterning of organic semiconductor films, as well as the resulting effects on charge transport in organic thin-film transistors, are explored. The presence of two or more anchoring sites between a halogenated semiconductor and a halogenated self-assembled monolayer, closer than about twice the corresponding van der Waals distance, alter the microstructure and improve electrical properties.

FULL PAPERS

A self-powered motion tracking system is developed to monitor the speed, direction, acceleration, starting and ending positions of a moving object, and even the moving path in one step in a two-dimensional system based on triboelectric nanogenerators (TENGs). This study opens a new area of TENGs with great application in self-powered systems, positioning detecting, motion tracking, environmental and infrastructure monitoring, and security.

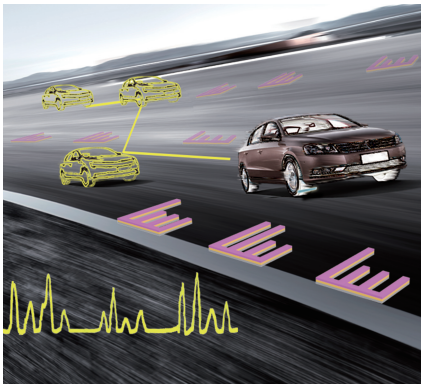

Motion Monitors

Triboelectric Nanogenerators as a Self-Powered Motion Tracking System

Fully printed transistors are demonstrated on paper substrates with performance on par with plastic based devices. Desirable paper properties such as foldability, breathability, and biodegradability are preserved outside of electronically active areas by an innovative locally printed smoothing process. This process is fully compatible with existing paper packaging process flows.

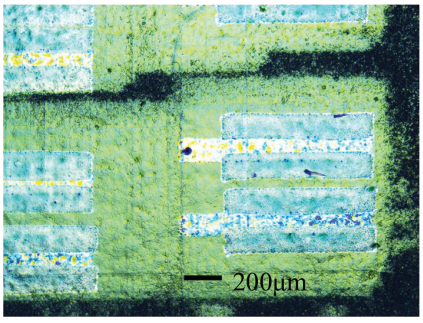

Organic Electronics

Printed Transistors on Paper: Towards Smart Consumer Product Packaging

Solution processing of Nb:TiO_2 has presented many challenges to the materials community. Nb:TiO_2 made by solution processing has been consigned to sensor/catalysis applications. Here, a solution route is presented to highly conductive and photocatalytically active Nb:TiO_2 films. A blue color is observed for the niobium doped films with XPS and computational methods showing a stable localized Ti^{3+} state at the anatase surface compared to the bulk.

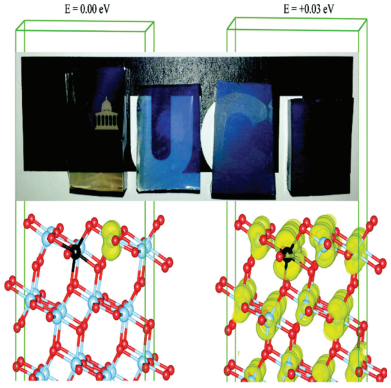

Thin Films

Solution Processing Route to Multifunctional Titania Thin Films: Highly Conductive and Photcatalytically Active Nb:TiO_2

A feasible method is reported for achieving a highly uniform, electroforming-free, and self-rectifying RS memory cell with a two-layered dielectric structure. HfO_2 works as the resistance switching layer by trapping and detrapping the deep 1.0 eV trap sites, whereas Ta_2O_5 layer remains intact during the switching and forms a high Schottky barrier with a high-work-function Pt to constitute the rectifying functionality.

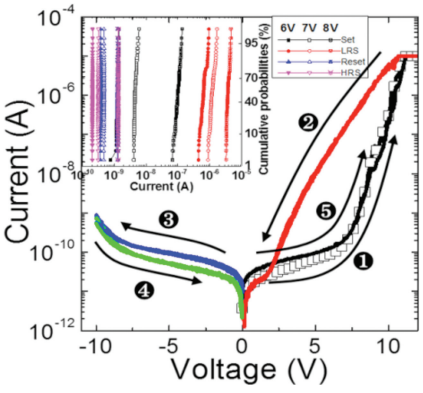

Resistive Switching

Highly Uniform, Electroforming-Free, and Self-Rectifying Resistive Memory in the Pt/Ta_2O_5/HfO_{2-x}/TiN Structure

FULL PAPERS

Microreactors

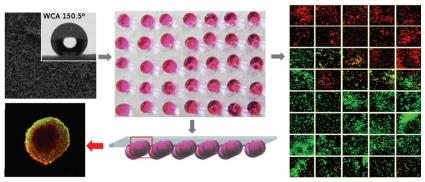

A lab-on-chip platform for high throughput screening of multiplexed and accelerated evaluations of physical, chemical, and biological processes is developed. The device permits the confinement and analysis of different combinations of elements and conditions in spherical, aqueous-based environments.

Supercapacitors

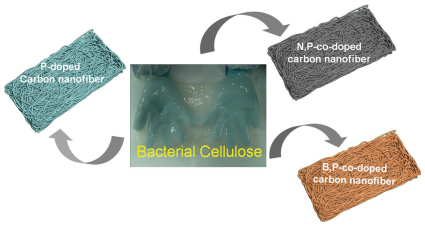

A simple, efficient, and general approach is developed for preparing cost-effective, three-dimensional, and large-scale heteroatom-doped carbon nanofibers, such as P-doped, N,P-co-doped, and B,P-co-doped carbon nanofibers, by pyrolyzing bacterial cellulose (BC) previously immersed in H_3PO_4, $NH_4H_2PO_4$, and H_3BO_3/H_3PO_4, respectively. Moreover, the as-prepared N,P-co-doped carbon nanofibers exhibit good supercapacitive performance.

Cathodes

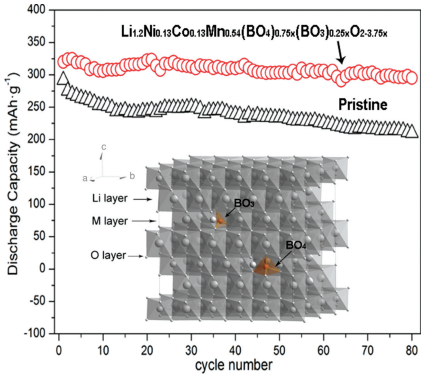

As-prepared $Li[Li_{0.2}Ni_{0.13}Co_{0.13}Mn_{0.54}](BO_4)_{0.015}(BO_3)_{0.005}O_{1.925}$ shows a decreased M-O covalency and a lowered O 2p band top compared with pristine $Li[Li_{0.2}Ni_{0.13}Co_{0.13}Mn_{0.54}]O_2$. As a result, the modified cathode exhibits a superior reversible capacity of 300 mA h g^{-1} after 80 cycles, excellent cycling stability with a capacity retention of 89% within 300 cycles, higher thermal stability, and enhanced redox couple potentials.

Graphene Oxide

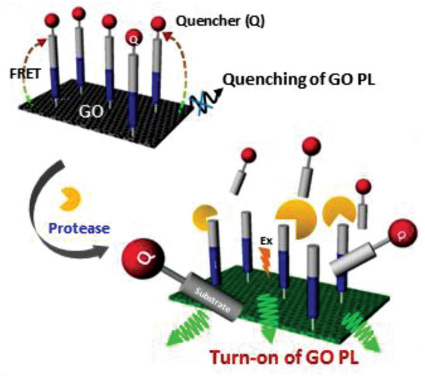

A graphene oxide (GO) fluorescence-based protease sensor consisting of a luminescent GO donor conjugated with a peptide-quencher complex detects cell-secreted proteases. The most effective quencher for GO fluorescence creates a GO–peptide–QXL optical sensor for protease detection. The quenched fluorescence of GO is restored by the proteolytic cleavage of a peptide quencher moiety from the sensor. This "turn-on" optical sensor detects MMP-2 secreted from live cells with high sensitivity.

FULL PAPERS

Solvent annealing in a selective solvent provides a method to invert the morphology of low bandgap polymer (LBG):fullerene mixtures from a polymer aggregate dispersed in a polymer:fullerene matrix to fullerene aggregates dispersed in a polymer:fullerene matrix. The judicious choice of solvent vapor provides a unique method to exquisitely control and optimize the morphology and performance of LBG:fullerene mixtures.

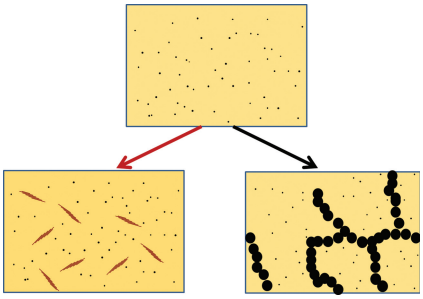

Heterojunctions

Unexpected high proton conduction inhighly dense sintered nano-TiO_2 electrolytes is explained by characterizing the open residual nanoporosity left behind by the fast pressure-assisted sintering method used. Solid-state ^1H NMR identifies two sites involved in proton conduction: H_2O confined in nanopores and –OH groups bonded to the nanopores walls. The effect of nanostructure on the enhanced proton conduction is discussed.

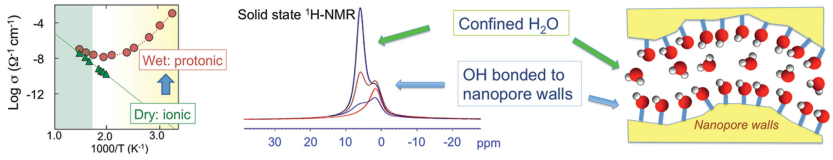

Proton Transport

Photochemical p- and n-doping of CVD-grown graphene is achieved using photoacid and photobase generators which do not themselves affect the electrical properties of the graphene, but which prime it for doping upon exposure to UV light. The doping level can be modulated by adjusting the exposure dose. This process tunes the Fermi level of the graphene sample.

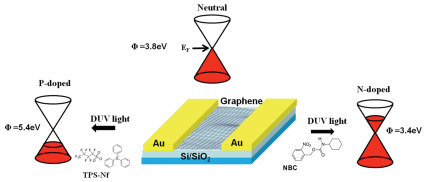

Graphene

Organic field effect transistors (OFETs) based on 2D graphene and hexagonal boron nitride heterostructures are fabricated by a dry-transfer method. The resulting heterostructured OFETs exhibit both high mobility and low operating voltage due to the atomically sharp interfaces of hBN flake and efficient charge carrier-injection from graphene electrodes.

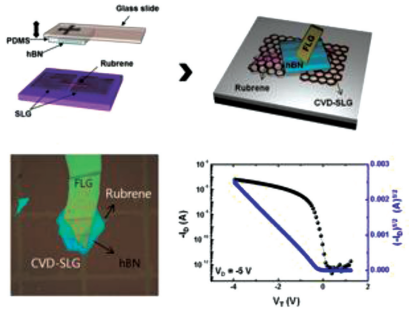

Organic Electronics